RAPID CURRENT TRANSITION IN A CROSSED-FIELD DIODE

by

J. P. Verboncoeur and C. K. Birdsall

Memorandum No. UCB/ERL M95/55

15 June 1995

RAPID CURRENT TRANSITION IN A CROSSED-FIELD DIODE

by

J. P. Verboncoeur and C. K. Birdsall

Memorandum No. UCB/ERL M95/55

15 June 1995

ELECTRONICS RESEARCH LABORATORY

College of Engineering
University of California, Berkeley
94720

Rapid Current Transition in a Crossed-Field Diode

J. P. Verboncoeur and C. K. Birdsall
Electronics Research Laboratory
University of California, Berkeley, CA 94720

June 1995

Abstract

The transmitted current in a crossed-field gap has been characterized analytically by a number of authors [1], [4], [6] and [7]. Using a one dimensional PIC simulation, PDP1 [9], we explore the behavior of the crossed-field diode at $B = B_{Hull}$. For mono-energetic (cold) emission, a rapid reduction of transmitted current is observed when the injected current exceeds the critical current by just 1%. Addition of a small electron temperature normal to the cathode eliminates the transition, even for $kT/V \sim 10^{-5}$ (V = 10 kV, gap = 1 cm, B = 337 G, $J = 1.69$ A/cm^2), while an isotropic velocity distribution accelerates the transition.

1 Background

Crossed-field planar and cylindrical electron diodes were first studied analytically and experimentally by Hull over 70 years ago [1]. The noise properties near cutoff have been studied by Pollack [2] and Van Duzer and Whinnery [3]. The Hull cutoff is well known; a summary appears in [4], drawing upon the work of Pollack. See also [5] and the references therein.

Recently, Lau, Christenson, and Chernin revived the study of the smooth-anode crossed-field diode [6]. Their analytic limiting current curve for planar diodes complements some of the older works [2]-[4]. Their limiting current analysis was for cold current injection, with electron velocity $v \to 0$ at the cathode.

2 Critical Point

This work is concerned with the critical point in the planar crossed-field diode. The critical point occurs at the Hull cutoff, $B = B_{Hull}$, with the injected current at the limiting (critical) current, $J = J_c$. For an idealized cold cathode, the Hull cutoff can be written

$$B_{Hull} = \frac{m}{ed}\sqrt{2eV/m + u_0^2}, \tag{1}$$

where u_0 is the electron velocity at the cathode, V is the gap voltage and d is the gap width.

At the Hull cutoff, the limiting current is given by $J_c/J_{CL} = 9/4\pi$ [2, 6], where J_{CL} is the Child-Langmuir limiting current for an unmagnetized diode with gap d and applied voltage V :

$$J_{CL} = \frac{4\epsilon_0}{9\sqrt{m/2e}}\frac{(V-V_m)^{3/2}}{(d-x_m)^2}\left(1 + \frac{2.66kT_e}{e(V-V_m)} + \ldots\right), \tag{2}$$

where kT_e is the electron temperature at the cathode, V_m is the minimum in potential, and x_m is the distance of the minimum measured from the cathode [8].

3 Simulation Results

The behavior of the smooth-electrode crossed-field diode at the critical point has been characterized using PDP1 [9], a one-dimensional electrostatic particle-in-cell simulation. During verification of the limiting current described by Lau [6], we discovered that the transmitted current at the critical point was very sensitive to the electron velocity at the cathode. In particular, a strong dependence on electron temperature and isotropy, injection current, and magnetic field was observed.

In this study, the anode voltage is V = 10 kV, and the gap width is d = 1 cm. The voltage source is an ideal battery of zero impedance connecting the anode to the cathode. The code requires a non-zero initial velocity for the injected electrons in order to avoid a singularity in charge density at the cathode. The initial velocity is $u_0 = 4.2 \cdot 10^5$ m/s, or 1/2 eV, small compared to the anode voltage. The resulting Hull cutoff is B_{Hull} = 337 G.

Case A. For injected electron current $J \leq J_c$, the diode is stable and all electrons are transmitted across the gap. Selected results for the critical point are shown by the solid curves in Fig. 1. The flow is laminar; each electron follows the same trajectory in phase space, and there are no measurable oscillations in the current, potential, or electron density. The transmitted current is equal to the injected current, up to J_c. At the critical point, the potential profile showed the spatial dependence $\Phi(x)/V = (x/d)^{1.47}$. In contrast, the potential profile of an unmagnetized current-limited diode ($J = J_{CL}$) is proportional to $x^{4/3}$.

Case B. Increasing the injected current to 1% above the critical value, the behavior changes dramatically, as shown by the dashed curves in Fig. 1. The temporal development of the current and potential follow that of the Case A until about 33 ns. Note, however, that the space charge in the gap exceeds that of Case A (Fig. 1e). At 33 ns, the current undergoes a rapid transition, dropping to 10% of the critical current. The transition occurs in about τ_{tran} =14 ns, and the transmitted current remains at $J_c/10$. Since $f_c\tau_{tran} = 13.2$, where f_c is the gyrofrequency, the transition is quite rapid. The flow is laminar prior to the transition, and becomes turbulent after (see Fig. 1d; later in time the hole in phase space collapses). The transmitted current and potential exhibit oscillations at the cyclotron frequency during the transition, which die out when the transition is complete. The noise level in the current increases significantly after the the transition (Fig. 1a). The potential profile in this case is proportional to $x^{1.78}$, so substantially more space charge is stored in the gap due to the recirculated electrons.

Case C. At injected currents $1.01J_c < J < J_{CL} = 4\pi J_c/9$, the behavior is similar to Case B. The duration of the transition and magnitude of the final transmitted current are relatively insensitive to the injected current. The onset of the transition occurs between 3.2-5.3 ns for $J \geq 1.1J_c$, compared to 33 ns at $J = 1.01J_c$. At currents above J_{CL}, the post-transition transmitted current declines slightly. The spatial and temporal evolution is similar to Case B shown in Fig. 1.

Case D. Next, the injected electrons were given a small anisotropic temperature, $kT_e = 1/10$ eV, normal to the cathode, in addition to a $\frac{1}{2}$ eV drift. The perpendicular temperature was zero. Since $kT_e \ll V$, the change in B_{Hull} due to the electron temperature is negligible. This thermal distribution has no effect on Case A, but at $J = 1.01J_c$ (Case B) the transition is does not occur; the diode exhibits stable, laminar behavior. The diode remains in this state indefinitely. Furthermore, the diode is also stable when retaining the anisotropic temperature, but eliminating the $\frac{1}{2}$ volt drift term.

Case E. Finally, an isotropic electron temperature, $kT_e = 1/10$ eV, was applied to the injected electrons for Case B. The combination of the isotropic temperature and the $\frac{1}{2}$ eV drift results in onset of the current transition in about 5 ns. The diode starts to oscillate much like a virtual cathode at about 10 ns, with a temporally decaying amplitude. A hole forms in $x-v_x$ phase space at the onset of the instability, much like Fig. 1d. This hole translates spatially, gradually collapsing by 100 ns. In the absence of the drift component of the injected electron velocity, the behavior is the same.

4 Conclusions

Rapid reduction of transmitted current is observed for a smooth-electrode vacuum crossed-field diode at the Hull cutoff when the injected current exceeds the critical current. The electron velocity distribution at the cathode plays a crucial role in the evolution of the transmitted current. Modifying the injection velocity distribution with a small anisotropic thermal component normal to the cathode eliminates the transition, while a small isotropic thermal component causes more rapid onset of the transition. The post-transition transmitted current is about 10% of the maximum transmitted current at the critical point, nearly independent of the injected current. The fluctuation level in the post-transition current (Fig. 1a) is significantly higher than than in the laminar diode due to the turbulence in phase space (Fig. 1d).

5 Acknowledgments

We are grateful to Y. Y. Lau and P. J. Christenson for generating stimulating discussions and assisting in this work. This research is supported by the Air Force Office of Scientific Research under grant F49620-92-J0487 and by the Office of Naval Research under grant number FD-N00014-90-J-1198.

References

[1] A. W. Hull, *Phys. Rev.*18, 31 (1921).

[2] M. A. Pollack, Ph.D. thesis, University of California, Berkeley, Series No. 60, Issue No. 485 (1962).

[3] T. Van Duzer and J. R. Whinnery, "Noise in Crossed-Field Electron Beams", in *Crossed-Field Microwave Devices*, Ed. E. Okress, Academic Press (1961).

[4] C. K. Birdsall and W. B. Bridges, *Electron Dynamics of Diode Regions*, Academic Press (1966).

[5] J. W. Gewartowski and H. A. Watson, *Principles of Electron Tubes*, D. Van Nostrand (1965). See esp. pp. 431-436.

[6] Y. Y. Lau, P. J. Christenson and D. Chernin, *Phys. Fl.* **5**, 4486 (1993).

[7] P. J. Christenson and Y. Y. Lau, *Phys. Plasmas* **1**, 3725 (1994).

[8] I. Langmuir, *Phys. Rev.* **21**, 419 (1923).

[9] J. P. Verboncoeur, V. Vahedi, M. V. Alves and C. K. Birdsall, *PDP1, PDC1, and PDS1: Plasma Device One-Dimensional Bounded Electrostatic Codes*, Plasma Theory and Simulation Group, University of California, Berkeley (1990). Available via http://ptsg.eecs.berkeley.edu.

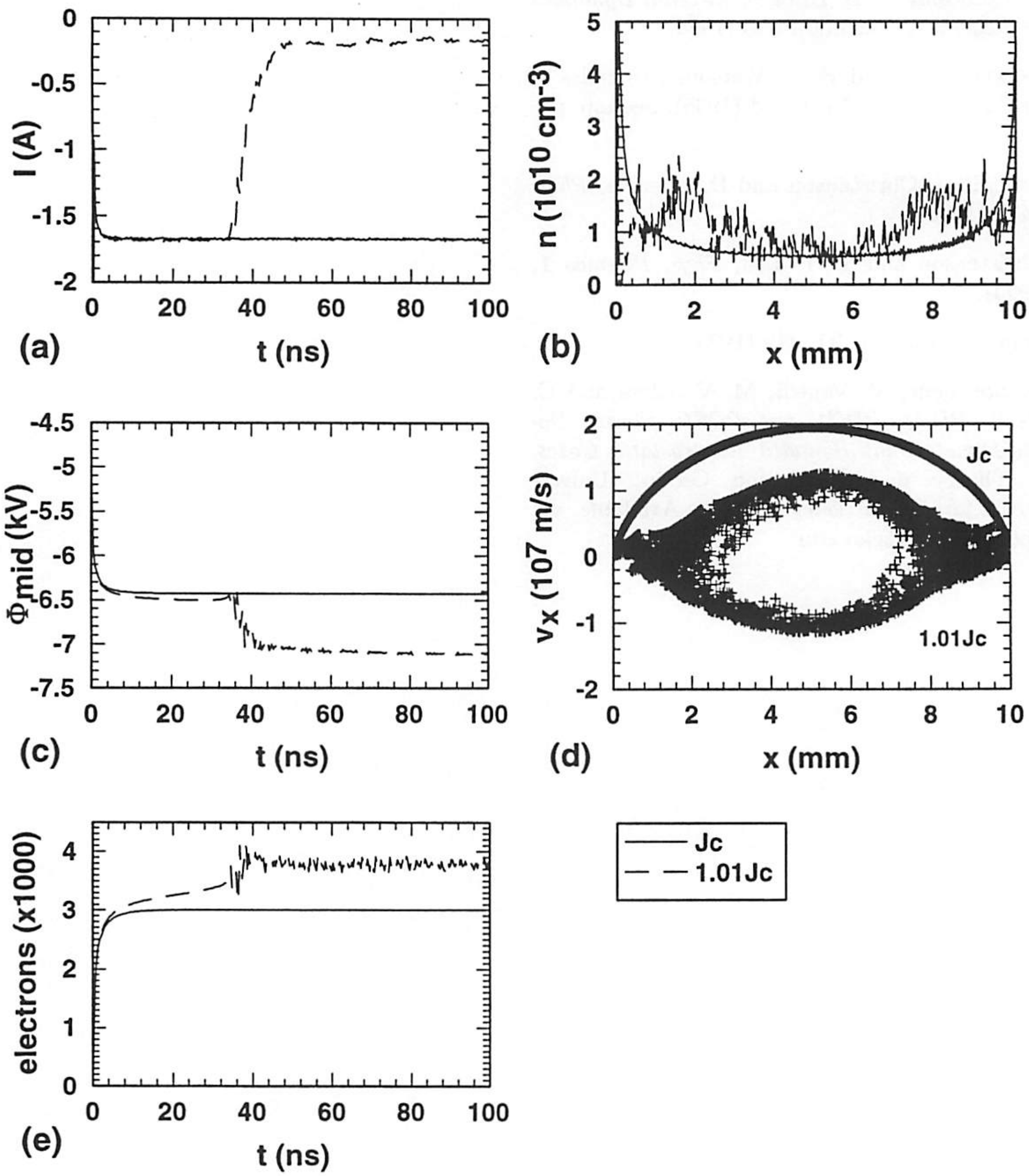

Figure 1: Crossed-field diode for Case A, the critical point (solid curves), and for Case B, at 1% above the critical point in injected current (dashed curves).

```
Hull Diode (IN MKS UNITS)
Injection of electron beam into a crossed field diode gap at high voltage.

-nsp---nc---nc2p---dt[s]---length[m]--area[m^2]--epsilonr---B[Tesla]---PSI[L]--
  1   400   3e6    5e-12      0.01        .0001      1.0       0.0337      90.0

-rhoback[C/m^3]---backj[Amp/m^2]---dde--extR[Ohm]--extL[H]---extC[F]--q0[C]-
    0.0                0.0          0.0    0.0       0.0       1.0     0.0

-dcramped--source--dc[V|Amp]--ramp[(V|Amp)/s]---ac[V|Amp]---f0[Hz]-theta0[D]-
  0          v      -10e3           0.0             0.0       1e7      0.0

--secondary---e_collisional---i_collisional---reflux---nfft--nsmoothing--ntimestep-
     0             0               0             0      512       0            0

--seec(electrons)---seec(ions)---ion species----Gpressure[Torr]---GTemp[eV]---
       0.0             0.2           2              5e-2            .026


ELECTRON-NEUTRAL COLLISIONAL PARAMETERS-----

--selsmax[m^2]---elsengy0[eV]---elsengy1[eV]---elsengy2[eV]-
       1.0e-19        0.0            0.0           10.0

--sextmax[m^2]---extengy0[eV]---extengy1[eV]---extengy2[eV]---
       1.0e-20       12.0            50.0            100.0

--sionmax[m^2]---ionengy0[eV]---ionengy1[eV]---ionengy2[eV]---
      1.0e-20        13.6         60.0            110.0

ION-NEUTRAL COLLISIONAL PARAMETERS-----

---achrgx[m^2]--bchrgx[m^2/V^1/2]-------ascat[m^2]--bscat[m^2/V^1/2]---
    3.0e-19        0.0                    2.0e-19        0.0


SPECIES 1

----q[C]-------m[Kg]---j0L[Amp/m^2]---j0R[Amp/m^2]----initn[m^-3]--
 -1.602e-19   9.11e-31    1.6687e4          0.0              0.0

--v0L[m/s]---v0R[m/s]---vtL[m/s]---vtR[m/s]----vcL[m/s]---vcR[m/s]-
   4.2e5      0.          0.0         0.0         0.0        0.0

---vperpt[m/s]---vperp0[m/s]---nbin----Emin[eV]----Emax[ev]---max-np--
     0.0            0.0         100       0.0         10e3      50000

-For-Mid-Diagnostic---nbin----Emin[eV]---Emax[eV]----XStart--XFinish--
                      100       0.0        15e3       .0045   .0055
```